Control Engineering Practice 46 (2016) 105–114

Contents lists available at ScienceDirect

Control Engineering Practice

journal homepage: www.elsevier.com/locate/conengprac

Nonlinear internal model controller design for wastegate control of a turbocharged gasoline engine ☆

Zeng Qiu [a,*], Jing Sun [b], Mrdjan Jankovic [c], Mario Santillo [c]

[a] Department of Electrical Engineering and Computer Science, University of Michigan, Ann Arbor, MI, USA
[b] Department of Navel Architecture & Marine Engineering, University of Michigan, Ann Arbor, MI, USA
[c] Ford Motor Company, Dearborn, MI, USA

ARTICLE INFO

Article history:
Received 17 February 2015
Received in revised form
1 September 2015
Accepted 19 October 2015

Keywords:
Internal model control
Wastegate control
Turbocharged gasoline engine
Quasi-linear parameter varying

ABSTRACT

Internal Model Control (IMC) has a great appeal for automotive powertrain control in reducing the control design and calibration effort. Motivated by its success in several automotive applications, this work investigates the design of nonlinear IMC for wastegate control of a turbocharged gasoline engine. The IMC design for linear time-invariant (LTI) systems is extended to nonlinear systems. To leverage the available tools for LTI IMC design, the quasi-linear parameter-varying (quasi-LPV) models are explored. IMC design through transfer function inverse of the quasi-LPV model is ruled out due to parameter variability. A new approach for nonlinear inversion, referred to as the structured quasi-LPV model inverse, is developed and validated. A fourth-order nonlinear model which sufficiently describes the dynamic behavior of the turbocharged engine is used as the design model in the IMC structure. The controller based on structured quasi-LPV model inverse is designed to achieve boost-pressure tracking. Finally, simulations on a validated high-fidelity model are carried out to show the feasibility of the proposed IMC. Its closed-loop performances are compared with a well-tuned PI controller with extensive feedforward and anti-windup built in. Robustness of the nonlinear IMC design is analyzed using simulations.

1. Introduction

Internal Model Control (IMC), whose diagram is shown in Fig. 1, is a well-established control design methodology with an intuitive control structure (Morari & Zafiriou, 1989). It incorporates a system model as an explicit element in the controller so that the control actions are determined based on the difference between the model output and the plant output. It has several desired features and closed-loop properties as established in Morari and Zafiriou (1989) and Garcia and Morari (1982), such as dual stability criterion, zero offset, and perfect control. The design, analysis, and implementation of IMC for linear systems have been well developed. Rivera, Morari, and Skogestad (1986) showed that process industrial IMCs for many SISO models can lead to PID controllers, occasionally augmented with a first-order lag. They also demonstrated the superiority of using IMC for PID tuning in terms of closed-loop performance and robustness.

The efficacy of IMC for nonlinear systems, however, has been investigated with limited comprehensive results. Economou, Morari, and Palsson (1986) presented an important result of nonlinear IMC, proving that the dual stability criterion, zero offset, and perfect control properties of LTI IMC would carry over to nonlinear cases. The IMC was implemented by finding a nonlinear dynamic inverse, which remained to be the key challenge in extending the IMC design to nonlinear systems. While the invertibility condition, inverse structure, and derivation for nonlinear dynamic system inverse were studied (Hirschorn, 1979), the derivation of the nonlinear inverse involved higher-order derivatives and caused problems when noises and disturbances were present in the system. In Economou et al. (1986), the nonlinear inverse was derived by exploiting the Hirschorn nonlinear inverse structure and solving it numerically using the contraction principle method or Newton's method. Stability of the IMC structure was discussed under the ideal circumstance that the model was the same as the plant. Henson and Seborg (1991) also exploited the result of Hirschorn nonlinear inverse for nonlinear IMC design. Several assumptions were made to calculate the higher-order derivatives. Feedforward/feedback linearization approach was adopted by Calvet and Arkun (1988) to derive the model for the nonlinear

☆This work is supported by Ford Motor Company.
* Corresponding author.
E-mail addresses: connieqz@umich.edu (Z. Qiu), jingsun@umich.edu (J. Sun), mjankov1@ford.com (M. Jankovic), msantil3@ford.com (M. Santillo).

http://dx.doi.org/10.1016/j.conengprac.2015.10.012
0967-0661/

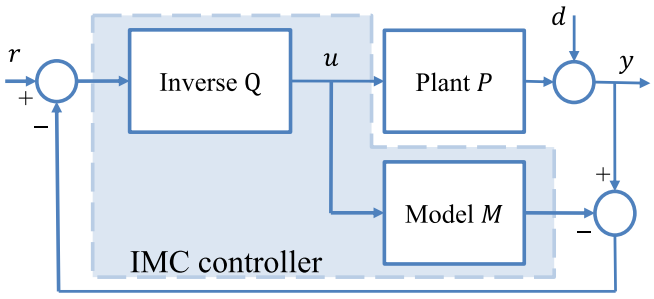

Fig. 1. Internal model control structure.

plant in IMC. Their approach accounted for the disturbances and input constraints.

Nonlinear IMC was also investigated in the adaptive control framework. Hunt and Sbarbaro (1991) used artificial neural networks for adaptive control of nonlinear IMC. Feasibility of identifying the nonlinear model and its inverse by a neural network was explored and demonstrated. Boukezzoula, Galichet, and Foulloy (2000) and Xie and Rad (2000) used fuzzy logic to estimate the model dynamics. The inverse was derived from this fuzzy model. The black-box identifications of neural network and fuzzy logic made it difficult to incorporate physical knowledge about the plant in the IMC design. In adaptive IMC scheme, using linear models to represent the dynamics of the nonlinear plant though adaptation has also been exploited (Brown, Lightbody, & Irwin, 1997; Datta, 1998; Shafiq, 2005).

Another possible avenue to exploit the linear IMC design tools for nonlinear systems would be through the linear parameter varying (LPV) model. Mohammapour, Sun, Karnik, and Jankovic (2013) applied IMC on a quasi-LPV model with two approaches. In the first approach, the IMC controller parameters were scheduled based on the LPV model parameters which were assumed to be known in real time and not vary rapidly. In the second approach, the design problem was formulated in the H_∞ framework as a set of linear matrix inequalities (LMI). Solving the associated LMI problem, however, was computationally intensive. Toivonen, Sandström, and Nyström (2003) derived the LPV model based on velocity-based linearization, then developed the IMC controller based on linear IMC theory. It was much less computationally demanding, but it was only applicable when there were a small number of scheduling parameters.

This paper explores nonlinear IMC for turbocharged gasoline engines driven by the need for developing robust and easy-to-calibrate powertrain control solutions and motivated by several successful industrial applications. IMC was first applied to turbocharged diesel engines for automotive applications. Alfieri, Amstutz, and Guzzella (2009) applied IMC based on the classical Smith predictor structure to air–fuel ratio control in turbocharged diesel engines with exhaust gas recirculation. Schwarzmann, Nitsche, and Lunze (2006) treated boost-pressure control of a turbocharged diesel engine with a variable nozzle turbine with IMC. Their IMC utilized a flatness-based approach to design the inverse Q, in which flatness means that the system inputs can be explicitly expressed in terms of internal system dynamics. In a follow up work, the same group also dealt with a two-staged turbocharged diesel engine using IMC (Schwarzmann, Nitsche, Lunze, & Schanz, 2006). The inverse Q was designed based on geometric nonlinear control design method. As turbocharged gasoline engines are becoming more popular, advanced control designs including IMC have been applied to turbocharged gasoline engines for improved performance. Thomasson, Eriksson, Leufven, and Andersson (2009) utilized IMC for PID tuning of wastegate control in turbocharged gasoline engines. Karnik and Jankovic (2012) later applied IMC directly to wastegate control for a turbocharged gasoline engine, motivated by the successful applications on turbocharged diesel engines. They used a first-order model which was simplified from a fourth-order nonlinear model using singular perturbation. While the simplicity of the first-order model-based design was an advantage for implementation, its performance was limited by the linear approximation, as it is defined for a particular operating point.

This work investigates the feasibility, performance, advantages, and limitations of a nonlinear IMC for automotive powertrain-control design, using the fixed geometry turbocharged gasoline engine as a case study. While the nonlinear dynamics of the system can be sufficiently described by a fourth-order model, inverting the nonlinear model for the IMC design represents the major challenge. To facilitate the IMC design, a quasi-LPV model (Rugh & Shamma, 2000) for the nonlinear model is developed. More importantly, the special quasi-LPV model structure is explored, and a structured quasi-LPV model is proposed, which leads to a feasible nonlinear inverse, referred to as the structured quasi-LPV inverse. The IMC based on the structured quasi-LPV inverse is developed, and its performance is analyzed. Simulation results, using a validated "virtual" plant model, are presented to demonstrate the effectiveness of the proposed design. This work is applicable to IMC with SISO nonlinear models of higher-order and is not limited by the number of scheduling parameters. The proposed IMC was originally presented as a conference paper (Qiu, Sun, Jankovic, & Santillo, 2014), whereas this paper represents an expanded version. More specifically, the design procedure is discussed in more detail from the stability point of view and robustness analysis is included.

The paper is organized as follows: Section 2 states the problem, presents two main tools used: IMC and LPV. Section 3 presents the nonlinear model for the turbocharged gasoline engine and exploits quasi-LPV approach to derive its inverse. Section 4 analyzes the IMC implementation results. Section 5 summarizes the paper.

2. Control problem and preliminaries

Gasoline engines have been aggressively downsized in an effort to reduce fuel consumption and CO_2 emissions. However, the torque provided by the engine is proportional to the air delivered to the cylinders. To meet the consumer demands for performance on the downsized engines, i.e., to maintain the engine output torque, turbochargers are widely adopted. They compress the intake air to increase the density of the engine airflow, thereby increasing the torque. The schematic of a turbocharged gasoline engine is shown in Fig. 2. The wastegate is the main actuator to control boost pressure. It affects the engine operation by changing the rotational speed of the turbine/compressor. The air is compressed by the compressor, and passes through an intercooler and a throttle before entering the engine intake port. The engine exhaust port is connected to the turbine, which is mechanically connected to the compressor. An electric wastegate actuator controls the opening of the turbine bypass path in this application (Karnik & Jankovic, 2012), affecting the compressor speed and therefore the boost pressure.

The turbocharged gasoline engine is expected to produce the desired engine torque, with higher fuel efficiency, power density, and lower emission (Guzzella & Onder, 2010). To achieve such goal, the desired engine torque is calculated from the driver pedal position. The desired engine torque is then mapped into desired intake manifold pressure and boost pressure considering the fuel economy and emission. These two pressures are then tracked through throttle and wastegate. This two input two output control problem can often be tackled with a decentralized controller:

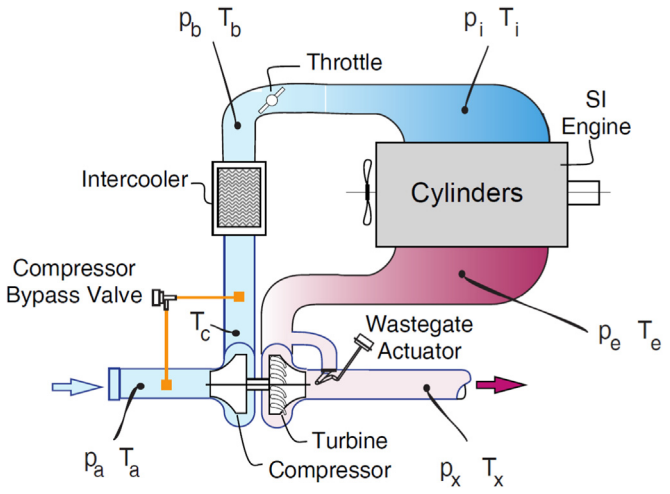

Fig. 2. System schematic of a turbocharged gasoline engine (Buckland, 2009).

using the throttle to track the intake manifold pressure and using the wastegate to track the boost pressure (Karnik, Buckland, & Freudenberg, 2005). In this paper, we will focus on using the wastegate to track the desired boost pressure, and the throttle is considered as an exogenous input. Boost pressure set-point tracking is a critical enabling technology for achieving improved fuel efficiency, power density, and emission reduction (Guzzella & Onder, 2010). However, operating conditions vary widely in automotive applications. This variation could result in inadequate boost at low speeds and loads, and over-boost situation at high speeds and loads. The wide range in operating conditions adds complexity to control design and calibration. IMC with a nonlinear model is adopted for its advantages in reducing the design and calibration effort.

A nonlinear IMC is developed in this paper for the control problem of boost-pressure tracking with the electric wastegate as the actuator. Measurements for boost pressure P_b, temperatures T_b, T_i, T_e, throttle opening u_{th}, and engine speed N_{en} are assumed to be available for feedback or feedforward control. The invertibility of the nonlinear model is assumed. To proceed with the design procedure of nonlinear IMC with structured quasi-LPV inverse, the preliminaries of IMC and quasi-LPV model are presented as below.

2.1. Internal model control

The schematic of a system with IMC is shown in Fig. 1, where P, M, and Q denote the plant, model, and inverse respectively. The IMC controller contains two elements: the inverse Q and the model M. Q takes the reference command and the difference between the outputs of the plant and the model as its inputs. If the model is exact, i.e., $M=P$, the IMC becomes a feedforward controller. Q is generally designed such that the norm of the difference e between the reference command r and the plant output y is minimized. Thus Q is chosen by solving

$$\min_{Q} \| e \|_2 = \min_{Q} \|(1 - QM)r \|_2, \tag{1}$$

subject to the constraint that Q is stable and casual. An absolute minimum could be reached at $Q = M^{-1}$ if M is invertible. However this is not feasible for a non-minimum phase (NMP) model, which is not stably invertible. An approximate inverse Q can be solved algebraically depending on the input r. Therefore, once the linear model is derived, the inverse of the model can be derived by solving the minimization problem (1). For a nonlinear model, however these tools are inapplicable, and effective approaches for inverting nonlinear models are very limited. Therefore, deriving

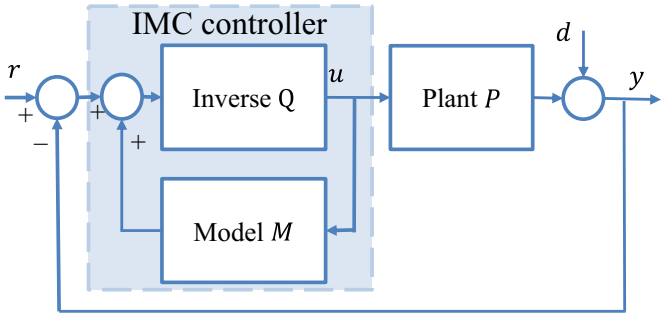

Fig. 3. Equivalent internal model control structure.

the model inverse is the main challenge and focus in this work. For both linear and nonlinear systems, once the model and its valid inverse are derived, IMC control design follows immediately. IMC have three main properties as established for LTI models (Garcia & Morari, 1982) and later extended to nonlinear cases (Economou et al., 1986):

(1) *Dual stability property*: When the model M is exact, stability of both inverse Q and plant P is sufficient for overall system stability.

(2) *Perfect control property*: By changing the position of the signal addition block in the IMC in Fig. 1, one can get an equivalent form of IMC as in Fig. 3, which has the same structure as the classical control. With this structure, the IMC controller can be presented by $Q(1 - MQ)^{-1}$, therefore, the sensitivity function of the IMC control system is $(1 - MQ)(1 - MQ + PQ)^{-1}$. When $MQ=1$, i.e., $Q = M^{-1}$, the sensitivity function is 0, which means "perfect control" is achieved.

(3) *Zero offset property*: A controller which satisfies $Q(0) = M(0)^{-1}$ adds integral action to the controller, and yields zero offset for a constant reference command r.

2.2. Quasi linear parameter varying model

Quasi-LPV models are LPV models for nonlinear systems where nonlinearities are hidden through state-dependent parameters, so that a nonlinear model can be represented by an LPV model and treated by LPV design techniques (Rugh & Shamma, 2000).

In general, a nonlinear model in the form of

$$\dot{x} = f(x, u) \tag{2}$$

can be expressed as an LPV model in the form of

$$\dot{x} = A(p)x + B(p)u \tag{3}$$

if the model (2) is affine in u and the time varying parameter vector p in (3) is allowed to be state-dependent to disguise the nonlinearities (Rugh & Shamma, 2000). For example, the nonlinear model

$$\dot{x}_1 = x_1^2 + x_1x_2, \quad \dot{x}_2 = \sin x_1 + u$$

can be expressed in quasi-LPV form as

$$\dot{x} = A(p)x + Bu = \begin{bmatrix} x_1 & x_1 \\ \frac{\sin(x_1)}{x_1} & 0 \end{bmatrix} x + \begin{bmatrix} 0 \\ 1 \end{bmatrix} u,$$

with $p = \left[x_1, \frac{\sin(x_1)}{x_1}\right]^T$, or

$$\dot{x} = A(p)x + Bu = \begin{bmatrix} x_1 + x_2 & 0 \\ \frac{\sin(x_1)}{x_1} & 0 \end{bmatrix} x + \begin{bmatrix} 0 \\ 1 \end{bmatrix} u,$$

with $p = \left[x_1 + x_2, \frac{\sin(x_1)}{x_1}\right]^T$.

In the next section, a nonlinear model for the turbocharged gasoline engine is presented. The quasi-LPV approach is exploited for representing it in a linear structure to aid deriving an inverse for the nonlinear model in IMC implementation.

3. Quasi-LPV model and its inversion

3.1. A nonlinear model for IMC design

Control-oriented models serve the IMC design and implementation in two different ways: first, the IMC incorporates a system model directly in its implementation as shown in Fig. 1; second, the standard IMC design procedure takes an inverse of the process model and augments it with a proper filter to avoid non-causal implementation to form the inverse Q.

The nonlinear model for the boost-pressure dynamics of a turbocharged engine presented in this paper is based on the work of Buckland (2009). The nonlinear model has the following states and one input:

$$x = [P_b, P_i, P_e, N_t]^T, \quad u = u_w,$$

where P_b is the boost pressure, P_i is the intake pressure, P_e is the exhaust pressure, N_t is the turbocharger speed, and the input u_w is the wastegate, which is the fraction of the opening and takes values in the range of [0, 1]. The dynamics of the pressures P_b, P_i, and P_e are derived using mass conservation along with isothermal manifold assumptions, while the dynamics of the turbocharger speed N_t are derived by a power balance between the turbine and the compressor as described in Karnik and Jankovic (2012) and Buckland (2009). The equations are summarized as follows:

$$\begin{aligned}
\frac{dP_b}{dt} &= \frac{RT_b}{V_b}(W_c - W_{th}),\\
\frac{dP_i}{dt} &= \frac{RT_i}{V_i}(W_{th} - W_{en}),\\
\frac{dP_e}{dt} &= \frac{RT_e}{V_e}\left(W_{en}\frac{1 + A/F}{A/F} - W_t - W_w\right),\\
\frac{dN_t}{dt} &= \frac{1}{I_t N_t}(H_t - H_c),
\end{aligned} \tag{4}$$

where R is the ideal gas constant, A/F is the air to fuel ratio, T, V, W, I and H are temperature, volume, mass flow rate, inertia, and power respectively. The subscript indicates the physical location of the variable as in Fig. 2, and b, c, th, i, en, e, t, and w are boost, compressor, throttle, intake, engine, exhaust, turbine, and wastegate respectively. Modeling of W (mass flow rate) and H (power) are described in detail in Karnik and Jankovic (2012) and Buckland (2009), and the resulting functional expressions are summarized as follows:

$$\begin{aligned}
W_c &= f_c\left(\frac{P_b}{P_a}, N_t\right),\\
W_{th} &= \frac{\mathrm{sat}(0, u_{th}, 1)}{\sqrt{RT_b}}\gamma P_b \phi\left(\frac{P_i}{P_b}\right),\\
W_{en} &= P_i \eta_{en}\frac{V_{en}}{RT_i}\frac{N_{en}}{2},\\
W_w &= \frac{\mathrm{sat}(0, u_w, 1)}{\sqrt{RT_e}}\gamma P_e \phi\left(\frac{P_x}{P_e}\right),\\
W_t &= f_t\left(\frac{P_e}{P_x}, \frac{N_t}{\sqrt{T_e}}\right)\frac{P_e}{\sqrt{T_e}},\\
H_t &= c_{p,e} T_e W_t \eta_t \psi_t, \quad \psi_t = 1 - \left(\frac{P_x}{P_e}\right)^{(\gamma_e - 1)/\gamma_e},\\
H_c &= c_{p,a} T_a W_c \frac{1}{\eta_c}\psi_c, \quad \psi_c = \left(\frac{P_b}{P_a}\right)^{(\gamma_a - 1)/\gamma_a} - 1,
\end{aligned} \tag{5}$$

where P_a is the ambient pressure, P_x is the turbine exit pressure, $\phi(\cdot)$ is a function of pressure ratio across the component, ψ is a mass flow parameter, γ is the specific heat ratio for air, $c_{p,(\cdot)}$ is the specific heat at constant pressure, η is the isentropic efficiency, u_{th} is the throttle opening, N_{en} is the engine speed, and $\mathrm{sat}(0, u, 1)$ limits u to be in the range [0, 1]. The temperatures T_b, T_i, and T_e are assumed to be measured. Typically the temperature sensors have a slow response time and delay, and the measurements are lead filtered to improve the response time. Therefore, the measurement inaccuracy is not considered in this work. A/F is the stoichiometric ratio of gasoline. u_{th} and N_{en} are considered as exogenous inputs in this work and they are measurable. All the variables and subscripts for the nonlinear model of turbocharged gasoline engine are summarized in Table 1.

The nonlinear model is evaluated by comparing its responses with those of the virtual "plant", which is a high fidelity Ford proprietary model that has been validated extensively. It includes the intercooler, throttle, engine, wastegate, turbine, and compressor (Buckland, 2009). Responses to a step change in the wastegate setting from 0.25 to 0.75 at $t = 5$ s for the nonlinear model and the virtual "plant" are shown in Fig. 4, confirming that the control-oriented nonlinear model and the "plant" have very similar dynamic responses.

Table 1
Nomenclature for modeling of turbocharged gasoline engine.

Variables		Subscripts	
A/F	Air to fuel ratio	a	Ambient
$c_{p,(\cdot)}$	Specific heat at constant pressure	b	Boost
$f_{(\cdot)}$	Compressor/turbine map	c	Compressor
I	Moment of inertia	e	Exhaust
N	Rotational speed	en	Engine
P	Pressure	i	Intake
H	Power	t	Turbine
R	Ideal gas constant	th	Throttle
T	Temperature	w	Wastegate
u	Fraction/degree of opening	x	Turbine exit
V	Volume		
W	Mass flow rate		
$\phi(\cdot)$	Function of pressure ratio across the component		
η	Isentropic efficiency		
ψ	Mass flow parameter		
γ	Ratio of specific heats		

3.2. Quasi-LPV turbocharged gasoline engine model

IMC control can be achieved by designing the inverse Q in Fig. 1 as the inverse of the model M. For linear models, their inverses can be achieved by inverting their transfer functions and appending a proper filter to assure causality. To extend this approach to nonlinear models, the quasi-linear parameter varying model approach is explored to represent the nonlinear model in a linear structure.

Note that there are an infinite number of quasi-LPV models in the form of (3) that can match (2), depending on the choice of the varying parameter p. For the turbocharged gasoline engine system, the physical couplings of state variables are considered and the following structure that leads to the most sparse A, B matrices is chosen:

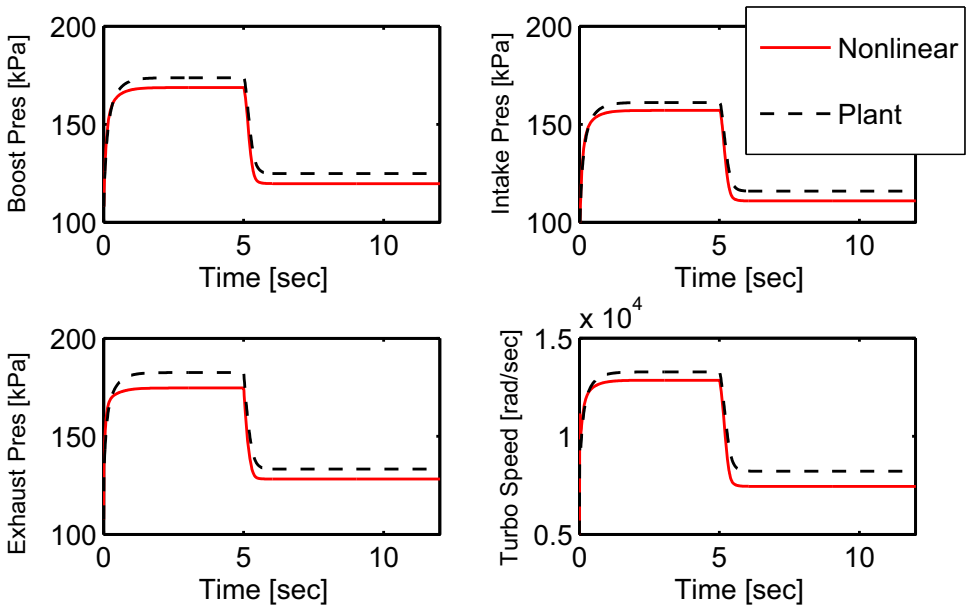

Fig. 4. Comparison of responses of the nonlinear model and the "plant" for a step change in wastegate actuation.

$$A=\begin{bmatrix} a_{11} & 0 & 0 & a_{14} \\ a_{21} & a_{22} & 0 & 0 \\ 0 & a_{32} & a_{33} & 0 \\ 0 & 0 & a_{43} & a_{44} \end{bmatrix}, \quad B=\begin{bmatrix} 0 \\ 0 \\ b_3 \\ 0 \end{bmatrix},$$

$$x=[P_b,\ P_i,\ P_e,\ N_t]^T, \quad u=u_w, \quad y=x_1. \tag{6}$$

The non-zero elements in (6) are defined as follows:

$$\begin{aligned}
a_{11} &= -\frac{RT_b}{V_b}\frac{W_{th}}{P_b} = -\frac{\sqrt{RT_b}}{V_b}\mathrm{sat}(0,\ u_{th},\ 1)\gamma\phi\left(\frac{P_i}{P_b}\right),\\
a_{14} &= \frac{RT_b}{V_b}\frac{W_c}{N_t} = \frac{RT_b}{V_bN_t}f_c\left(\frac{P_b}{P_a},\ N_t\right),\\
a_{21} &= \frac{RT_i}{V_i}\frac{W_{th}}{P_b} = \frac{RT_i}{V_i}\frac{\mathrm{sat}(0,\ u_{th},\ 1)A_{max}}{\sqrt{RT_b}}\phi\left(\frac{P_i}{P_b}\right)\gamma,\\
a_{22} &= -\frac{RT_i}{V_i}\frac{W_{en}}{P_i} = -\frac{RT_i}{V_i}\frac{V_{en}N_{en}}{2RT_i},\\
a_{32} &= \frac{1+A/F}{A/F}\frac{RT_e}{V_e}\frac{W_{en}}{P_i} = \frac{1+A/F}{A/F}\frac{T_e\eta_{en}V_{en}N_{en}}{2V_eT_i},\\
a_{33} &= -\frac{RT_e}{V_e}\frac{W_t}{P_e} = -\frac{R\sqrt{T_e}}{V_e}f_t\left(\frac{P_e}{P_x},\ \frac{N_t}{\sqrt{T_e}}\right),\\
a_{43} &= \frac{H_t}{I_tN_tP_e} = \frac{1}{I_tN_t}c_{p,e}T_e\frac{W_t}{P_e}\eta_t\psi_t,\\
a_{44} &= -\frac{H_c}{I_tN_t^2} = -\frac{1}{I_tN_t^2}c_{p,a}T_aW_c\frac{1}{\eta_c}\psi_c,\\
b_3 &= -\frac{RT_e}{V_e}\frac{W_w}{\mathrm{sat}(0,\ u_w,\ 1)} = -\frac{\sqrt{RT_e}}{V_e}\gamma P_e\phi\left(\frac{P_x}{P_e}\right).
\end{aligned} \tag{7}$$

3.3. Structured quasi-LPV inverse

Given that the parameters defined by (7) are varying fast during transients, treating the parameters as frozen and deriving the transfer function of (6) will not be effective for deriving the inverse. Indeed, by numerical simulations it is confirmed that the transfer function inverse does not represent the nonlinear model inverse. In this section, the special form of the quasi-LPV structure of (6) is explored to derive its inverse model in an effort to minimize the approximation error.

(1) *Quasi-LPV model inverse structure*: Exploiting the sparsity of the A, B matrices of model (6), the quasi-LPV model is expressed as an integration of several first-order sub-models. With this very special structure of the nonlinear model, the inverse can be pursued by deriving the inverse of multiple first order nonlinear models, which will involve limited approximation.

Given the sparse matrices A, B in the form of (6), the following first-order sub-models Σ_1, Σ_2, Σ_3, Σ_4 are defined as

$$\begin{aligned}
&\Sigma_1\colon \dot{x}_1 = a_{11}x_1 + a_{14}x_4 \Longrightarrow x_1 = \Sigma_1(x_4),\\
&\Sigma_2\colon \dot{x}_2 = a_{22}x_2 + a_{21}x_1 \Longrightarrow x_2 = \Sigma_2(x_1),\\
&\Sigma_3\colon \dot{x}_3 = a_{33}x_3 + a_{32}x_2 + b_3u \Longrightarrow x_3 = \Sigma_3(x_2,\ u),\\
&\Sigma_4\colon \dot{x}_4 = a_{44}x_4 + a_{43}x_3 \Longrightarrow x_4 = \Sigma_4(x_3).
\end{aligned} \tag{8}$$

Further expressing Σ_3 to be

$$\Sigma_3(x_2,\ u) = \Sigma_{31}(x_2) + \Sigma_{32}(u),$$

we can show that the input–output relation of the quasi-LPV model can be expressed as a composition of these sub-models:

$$y = x_1 = \Sigma_1(\Sigma_4(\Sigma_3(\Sigma_2(x_1),\ u))) = \Sigma_1(\Sigma_4(\Sigma_{31}(\Sigma_2(x_1)) + \Sigma_{32}(u))), \tag{9}$$

whose block diagram representation is shown in Fig. 5.

Expressing the input u in terms of the output y based on (9),

$$u = \Sigma_{32}^{-1}(\Sigma_4^{-1}(\Sigma_1^{-1}(y)) - \Sigma_{31}(\Sigma_2(y))), \tag{10}$$

which can be viewed as an inverse model of (9). Fig. 6 shows the block diagram representation of the inverse of the quasi-LPV model through the integration of several inverse models of first-order blocks as expressed in (10), in which $\overline{\Sigma_1^{-1}}$, $\overline{\Sigma_4^{-1}}$, and $\overline{\Sigma_{32}^{-1}}$ are approximate inverses of Σ_1, Σ_4, and Σ_{32}. The derivations of the $\overline{\Sigma_1^{-1}}$, $\overline{\Sigma_4^{-1}}$, and $\overline{\Sigma_{32}^{-1}}$ are explained in the following section. $\overline{x_1}$–$\overline{x_4}$ in Fig. 6 are approximations of x_1–x_4 in Fig. 5.

(2) *First-order quasi-LPV inverse*: We now derive the inverse of the first-order quasi-LPV model and define its property in order to derive the representation for the inverse model (10).

For a first-order quasi-LPV model:

$$\Sigma_i\colon \dot{x} = ax + bu, \tag{11}$$

define

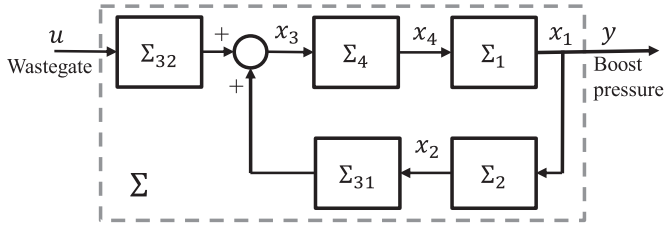

Fig. 5. Interconnection of the first-order quasi-LPV sub-models for the fourth-order turbocharged gasoline engine LPV model.

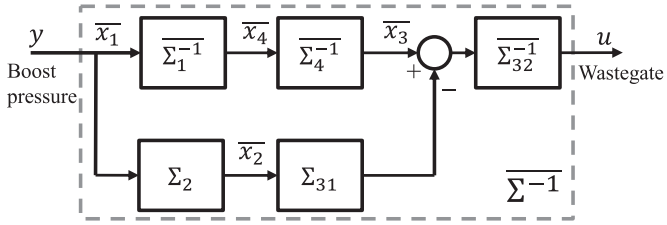

Fig. 6. Interconnection of first-order quasi-LPV sub-models for inverse of the LPV model shown in Fig. 5.

$$\bar{u} = \left\{\frac{1}{\tau s+1}\right\}u, \tag{12}$$

where $\{\frac{1}{\tau s+1}\}$ denotes the first-order filter with a transfer function $\frac{1}{\tau s+1}$. Then, the following lemma gives the representation of $\bar{u}$.

Lemma 1. *Let a, b be time varying parameters with $a, b \in \mathcal{L}_\infty$, $b \neq 0$, and $b \in C^1$. Then, for any u, $\bar{u}$ given by (12) can be expressed in terms of the state x as*

$$\begin{aligned}\bar{u} &= \frac{1}{\tau b}x - z,\\ \dot{z} &= \frac{1}{\tau}\left(-z + \left(\frac{1}{b\tau} - \frac{\dot{b}}{b^2} + \frac{a}{b}\right)x\right),\end{aligned} \tag{13}$$

where x is given by (11).

Proof. Note that

$$\bar{u} = \left\{\frac{1}{\tau s+1}\right\}u = \left\{\frac{1}{\tau s+1}\right\}\left(\frac{\dot{x}}{b} - \frac{ax}{b}\right). \tag{14}$$

Since

$$\frac{d}{dt}\left(\frac{x}{b}\right) = \frac{\dot{x}}{b} - \frac{\dot{b}x}{b^2}, \tag{15}$$

we have, from (14), that

$$\begin{aligned}\bar{u} = \left\{\frac{1}{\tau s+1}\right\}\left(\frac{d}{dt}\left(\frac{x}{b}\right) + \frac{\dot{b}x}{b^2} - \frac{ax}{b}\right) &= \left\{\frac{1}{\tau s+1}\right\}\{\tau s+1\}\left(\frac{x}{\tau b}\right)\\ &- \left\{\frac{1}{\tau s+1}\right\}\left[\left(\frac{1}{b\tau} - \frac{\dot{b}}{b^2} + \frac{a}{b}\right)x\right].\end{aligned} \tag{16}$$

Note that the time invariant operator $\{\tau s+1\}$ can now be canceled with $\{\frac{1}{\tau s+1}\}$ since there is no time varying signal in between. Let

$$z = \left\{\frac{1}{\tau s+1}\right\}\left[\left(\frac{1}{b\tau} - \frac{\dot{b}}{b^2} + \frac{a}{b}\right)x\right], \tag{17}$$

then the dynamics from output x to $\bar{u}$ can be represented by a first-order LPV model

$$\begin{aligned}\bar{u} &= \frac{1}{\tau b}x - z,\\ \dot{z} &= \frac{1}{\tau}\left(-z + \left(\frac{1}{b\tau} - \frac{\dot{b}}{b^2} + \frac{a}{b}\right)x\right).\ \square\end{aligned} \tag{18}$$

Remark 1. Treat x as the input, $\bar{u}$ as the output, and a, b, and τ as the parameters, the BIBO stability of the first order system (13) can be easily established given that the system has a single frozen-time pole at $-\frac{1}{\tau}$, and $\frac{1}{\tau b}$, $\frac{1}{\tau}(\frac{1}{b\tau} - \frac{\dot{b}}{b^2} + \frac{a}{b})$ are bounded.

Remark 2. Note that since $\bar{u} \approx u$ for small τ, one can treat (13) as an approximate inverse model of (11). Moreover, $|\bar{u} - u| \propto O(\tau)$, namely, the inverse model error can be made arbitrarily small with a properly chosen τ.

Remark 3. Lemma 1 assumes a continuous-time implementation of the inverse of (11). When (13) is discretized for real engine implementation, its BIBO stability remains due to Remark 1. If the delay caused by discretization is small, its performance will not be substantially affected.

Now the approximate inverse model $\overline{\Sigma_i^{-1}}$ is given by (13). For simplicity, one can drop the $\dot{b}/b^2$ term if the parameter variation is substantially slower than the system dynamics. However, this is not the case in this application. $\dot{b}/b^2$ as in (7) includes the states. Therefore, $\dot{b}/b^2$ is not slower than the system dynamics. The following simulation also verified that $\dot{b}/b^2$ should not be omitted: To validate the first-order sub-model inverse, the two systems Σ_i and $\overline{\Sigma_i^{-1}}$ are connected in cascade as shown in Fig. 7. According to Remark 2, the output v in Fig. 7 should be close to the input $\bar{v}$. A numerical analysis of the inverse performance is shown in Fig. 8. It is obvious that the inverse incorporating the $\dot{b}/b^2$ term with smaller time constant τ has better accuracy. Therefore, the inverse incorporating $\dot{b}/b^2$ is adopted in the subsequent derivation. The time constant τ is the tuning parameter for the IMC design. Fig. 8 indicates that smaller time constants lead to a better inverse, as expected.

(3) *Structured quasi-LPV inverse*: Representing each first-order model inverse in (10) with (13), an inverse model for the nonlinear model is derived, which will be referred to as the structured quasi-LPV inverse.

To incorporate the quasi-LPV inverse model in the IMC structure, two implementable configurations are possible as shown in Figs. 9a and b. Firstly, one can use the states in the nonlinear model Σ to schedule the parameters in the inverse model $\overline{\Sigma^{-1}}$ (as in Fig. 9a). Since the states used for parameter scheduling are external to $\overline{\Sigma^{-1}}$, Fig. 9a is referred to as the externally scheduled quasi-LPV inverse. Secondly, since all the states in the original quasi-LPV model are explicit in its inverse structure, one can derive parameters used in A and B (defined in (6)) for $\overline{\Sigma^{-1}}$ based on the internal states in $\overline{\Sigma^{-1}}$ (as in Fig. 9b), which is referred to as the internally scheduled quasi-LPV inverse.

While the externally scheduled quasi-LPV inverse looks appealing at first, its utility is ruled out after more in-depth analysis and simulation. The dashed line in Fig. 9a which represents the gain scheduling signal forms a feedback loop, which causes instability. In this work, the proposed IMC controller uses the internally scheduled quasi-LPV inverse model for its implementation. It should be noted that the internally scheduled quasi-LPV inverse is not possible for inverse LPV model derived by general

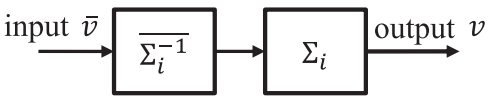

Fig. 7. Structure for validation of first-order inverse.

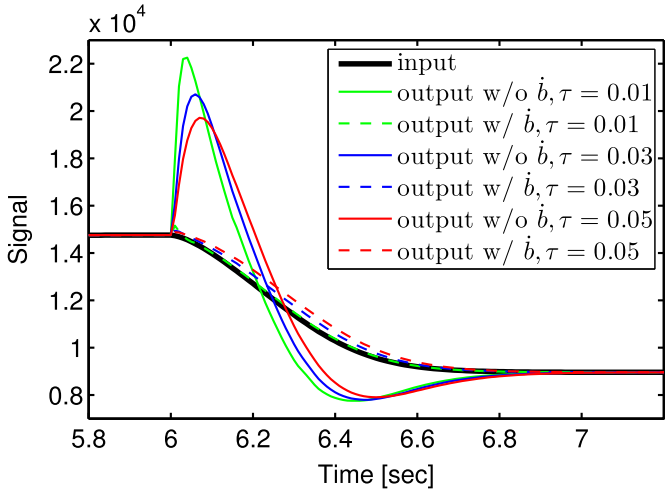

Fig. 8. Analysis of first-order inverse $\overline{\Sigma_1^{-1}}$ with and without $\dot{b}$ ($\dot{b}$ is derived from numerically differentiating b).

system inverting methodologies, unless the states are preserved in the inverse model. With the structured quasi-LPV inverse model shown in Fig. 6, it is true that all states are explicitly preserved in the inverse model, thereby making the internally scheduled quasi-LPV inverse implementation possible.

(4) *Stability of the structured quasi-LPV inverse*: Even though each subsystem in the structured quasi-LPV model is BIBO stable, the overall inverse $\overline{\Sigma^{-1}}$, with internally scheduled parameters, still has stability issues due to the feedback loop introduced by those state-dependent parameters.

Since the state-dependent parameters are the root cause for the instability phenomenon in the structured quasi-LPV inverse model, an in-depth analysis of the parameter scheduling is carried out in the inverse model. Fig. 10 shows the scheduling of the varying parameters in each sub-model for the internally scheduled quasi-LPV inverse. One can see that some of the interconnections, shown by the blue solid lines in Fig. 10 from the states $\overline{x}_1$ and $\overline{x}_2$, do not introduce additional feedback loops except those within their own sub-models. Others, that are shown by red dotted line for the parameters scheduled based on $\overline{x}_3$ and $\overline{x}_4$, form additional feedback loops within the structured quasi-LPV inverse. Meanwhile, the errors from $\overline{\Sigma_1^{-1}}$, $\overline{\Sigma_4^{-1}}$, and $\overline{\Sigma_{32}^{-1}}$ propagate within the structure, leading to complicated dynamic responses. To construct a stable inverse, the scheduling signals $\overline{x}_3$ (approximate exhaust pressure) and $\overline{x}_4$ (approximate turbo speed) are replaced by their steady-state values. The steady-state maps are generated with respect to different engine speed and throttle opening.

Remark 4. Note that, based on the dual stability property of IMC (Garcia & Morari, 1982), the stability of the closed-loop system can be assured if P and Q are stable and $M=P$. The stability of the quasi-LPV inverse Q can be established given that it is made up by stable sub-models Σ_i's and $\overline{\Sigma_i^{-1}}$'s through feedforward connections. All feedback loops in Q are eliminated after replacing the

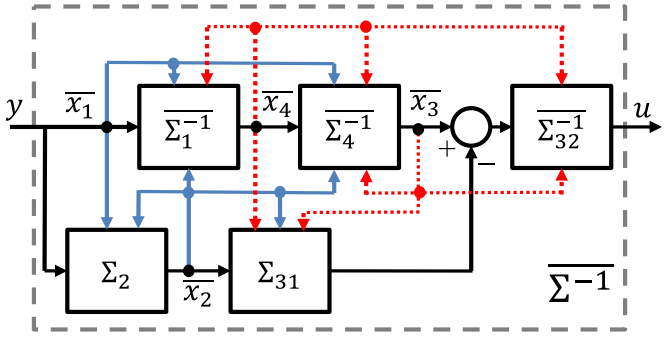

Fig. 10. Parameter scheduling relationship in the internally scheduled quasi-LPV inverse (blue solid lines indicate that the states are actually used for scheduling; red dotted lines represent the use of the steady state value generated from steady state mapping in scheduling). (For interpretation of the references to color in this figure caption, the reader is referred to the web version of this paper.)

gain-scheduling elements that form feedback loops using their steady state values. Therefore, the stability of the closed-loop system with IMC can be assured using $Q = \overline{\Sigma^{-1}}$ given in Fig. 10.

(5) *Structured quasi-LPV inverse model validation*: The inverse model shown in Fig. 10, with some of the state-dependent parameters replaced by steady-state mapping values, is validated through simulation. The validation is performed by connecting the inverse to the original model as in Fig. 9b and the validated results are shown in Fig. 11.

Note that the quality of the inverse model depends on the tuning parameters, which are the time constants τ as in each first-order LPV sub-model inverse $\overline{\Sigma_1^{-1}}$, $\overline{\Sigma_4^{-1}}$, and $\overline{\Sigma_{32}^{-1}}$ as shown in Fig. 6. Theoretically if the time constants are small, the output has faster responses but also potential oscillations during transients. If the time constants are large, the transient response will be slow. Two results with different tuning parameters are shown in Fig. 11, which validates the inverse model. Inverse 1 has the time constants 0.1 s, 0.04 s, and 0.02 s in $\overline{\Sigma_1^{-1}}$, $\overline{\Sigma_4^{-1}}$, and $\overline{\Sigma_{32}^{-1}}$, respectively. Inverse 2 has the time constants 0.05 s, 0.04 s, and 0.02 s in $\overline{\Sigma_1^{-1}}$, $\overline{\Sigma_4^{-1}}$, and $\overline{\Sigma_{32}^{-1}}$, respectively. Inverse 1, which has the larger time constant, is more damped than inverse 2 and has little overshoot, which matches the intuition. The time constant for $\overline{\Sigma_1^{-1}}$ is chosen to be larger than the others, considering the error in its output $\overline{x}_4$ propagates to $\overline{x}_3$ and u, as shown in Fig. 10.

4. Performance evaluation of IMC on turbocharged gasoline engine

With the fourth-order nonlinear model and the model inverse developed, IMC can be designed by applying the nonlinear model and its inverse into Fig. 1. The IMC is implemented in continuous-time domain, and is applied to the virtual "plant", which is a validated Ford proprietary model. The structure of the resulting nonlinear IMC system is shown in Fig. 12. The tuning parameters are the time constants in each first-order LPV sub-model inverse

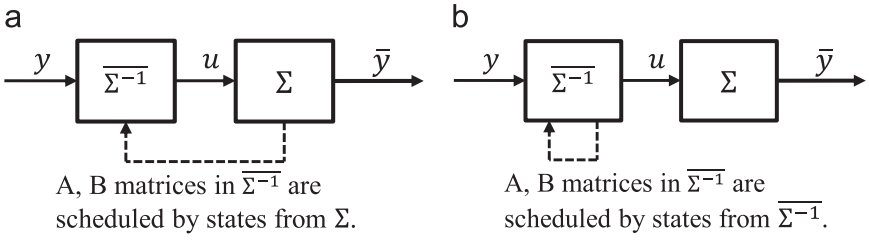

Fig. 9. Validation structures: (a) externally scheduled quasi-LPV inverse validation structure and (b) internally scheduled quasi-LPV inverse validation structure.

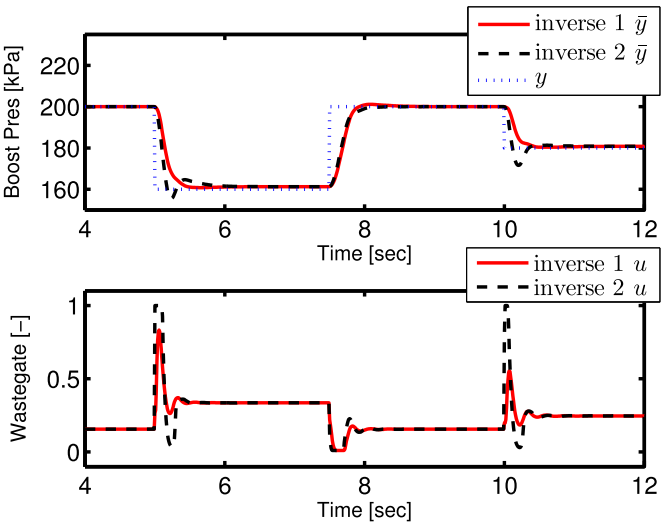

Fig. 11. Validation of structured quasi-LPV inverse.

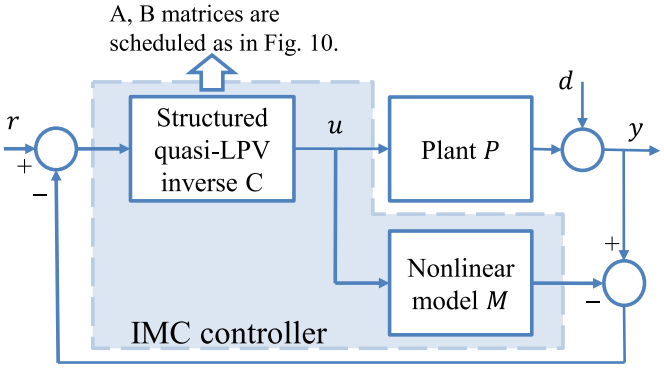

Fig. 12. IMC structure with structured quasi-LPV inverse.

$\overline{\Sigma_1^{-1}}$, $\overline{\Sigma_4^{-1}}$, and $\overline{\Sigma_{32}^{-1}}$, as shown in Fig. 6. The time constants are chosen at 0.1 s, 0.04 s, and 0.02 s, which are the same as in inverse 1. The pressure and temperature sensors are assumed to be accurate. Performance of the resulting control system is evaluated in this section together with the robustness analysis with respect to different operating conditions and measurement noises.

4.1. Performance evaluation

To evaluate the performance of IMC, some features have to be considered (Moulin & Chauvin, 2011):

- The overshoot of P_b has to be minimized to avoid throttle reclosing.
- The pressure oscillation of P_b while tracking a step function is undesirable because they could generate torque oscillations that are noticeable to the driver.

IMC is compared with a well-tuned PI controller with extensive feedforward and anti-windup built in, which is referred to as PI control in the context. The system response and control input are compared in two cases: constant engine speed of 3000 rpm (as in Fig. 13a); varying engine speed (as in Fig. 13b). Here varying engine speed rises from 1500 to 3000 rpm gradually. The throttle opening is 45° in both simulations. In Fig. 13a, it can be observed that IMC achieved a faster reference tracking than PI with less overshoot or oscillation. In Fig. 13b, the IMC response does not overshoot, even without incorporating an explicit anti-windup strategy.

Overall, the nonlinear IMC for the wastegate control of a turbocharged gasoline engine shows promising performance. It shows good reference tracking, no steady-state error, no need for a separate anti-windup design, and intuitive tuning. Its performance matches, and in cases exceeds, that of a well-tuned PI control with extensive feedforward and anti-windup built in.

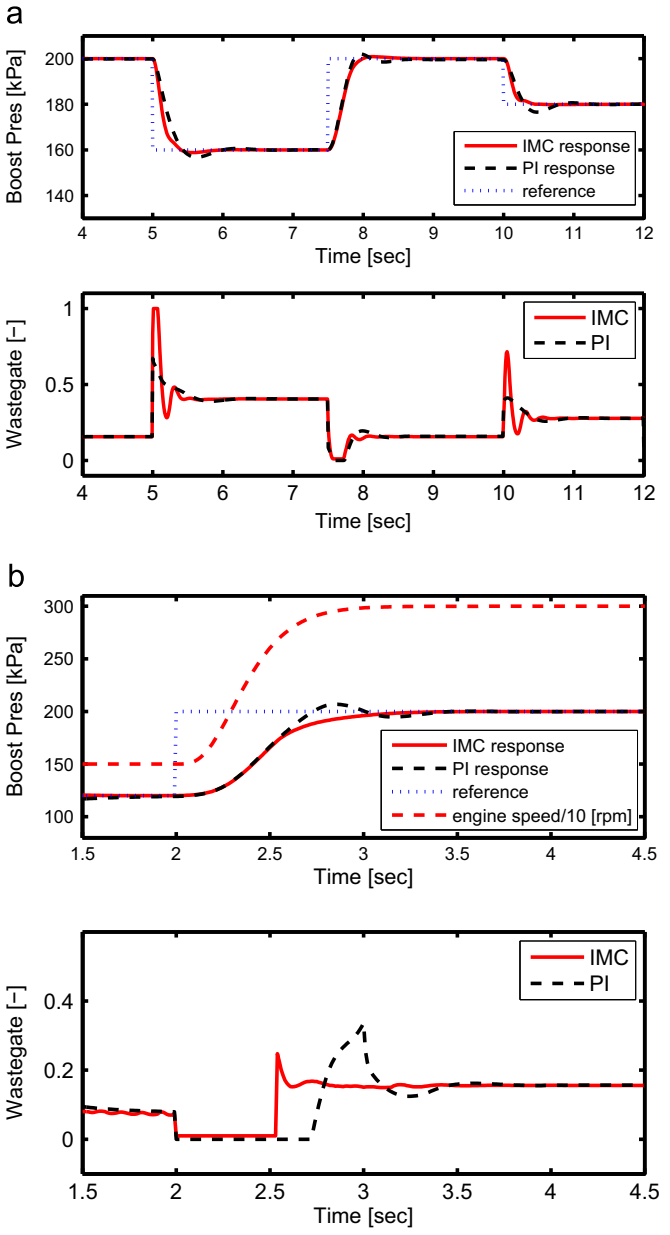

Fig. 13. Simulation results. (a) IMC performance: constant engine speed. (b) IMC performance: varying engine speed.

4.2. Performance in the presence of disturbances

In real applications of boost-pressure control of a turbocharged gasoline engine, the reference and operating points vary. More analysis is performed herein to evaluate the system performance sensitivity with respect to the variation of operating conditions (engine speed and throttle opening). Note that only one set of tuning parameters is used for all the tests.

First, the impact of the engine speed N_{en} is considered. Two sets of tests are performed: the same P_b reference step at different engine speed N_{en} (as in Fig. 14a), constant P_b reference with a step change in N_{en} (as in Fig. 14b), in which case the variation in N_{en} can

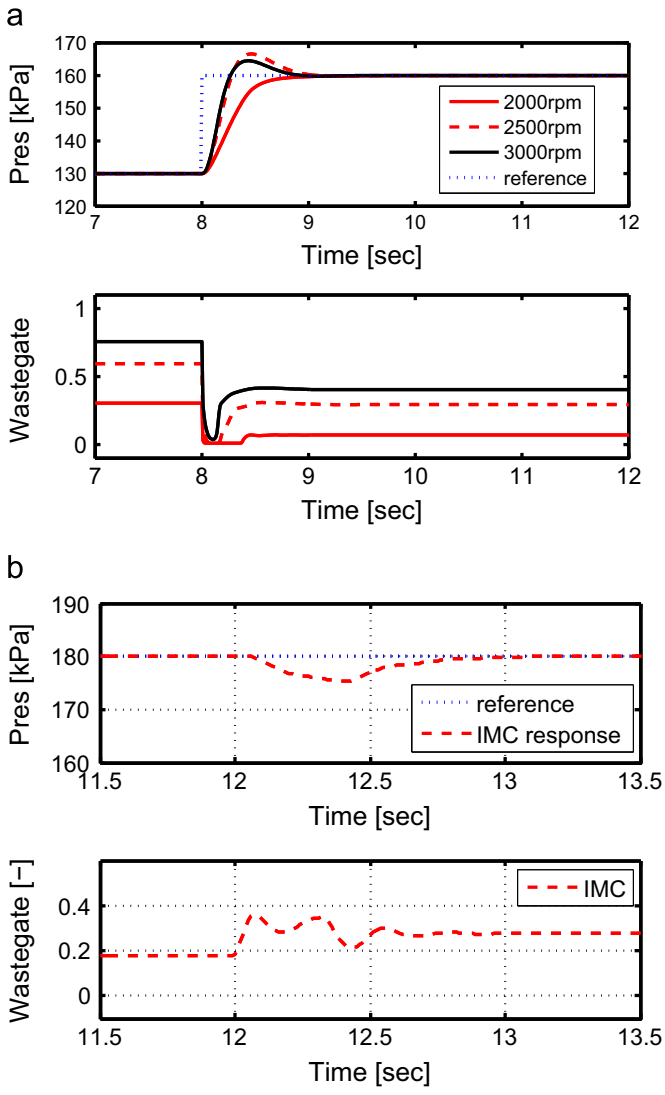

Fig. 14. IMC robustness evaluation with respect to engine speed. (a) IMC robustness: different engine speed. (b) IMC robustness: varying engine speed, constant reference.

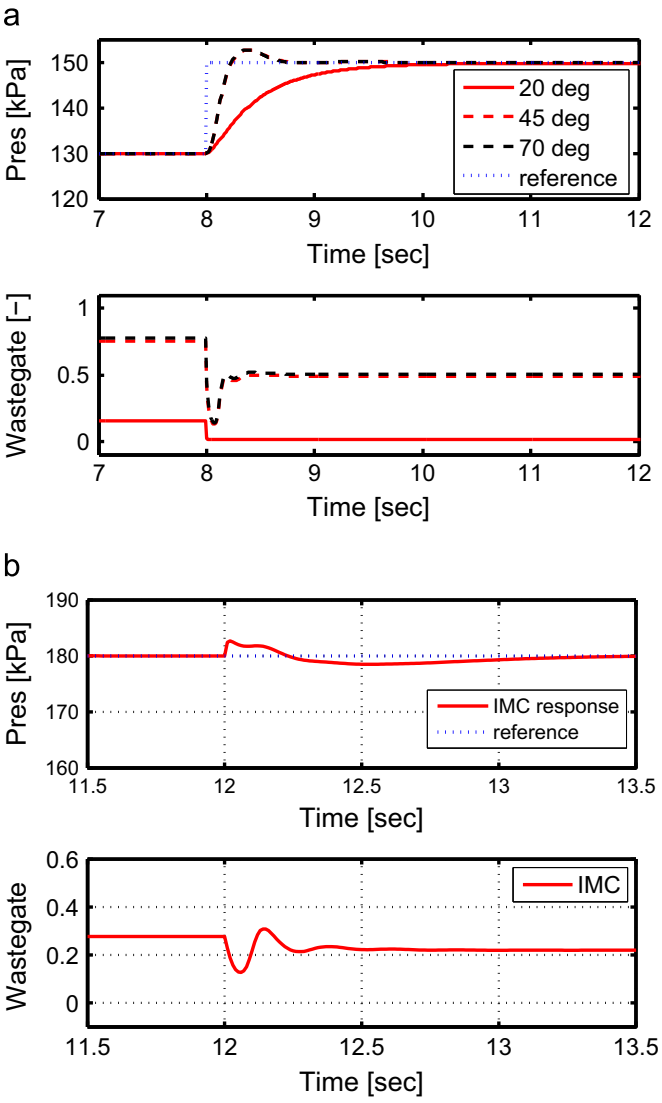

Fig. 15. IMC robustness evaluation with respect to throttle opening. (a) IMC robustness: different throttle opening. (b) IMC robustness: step change in throttle opening, constant reference.

be viewed as a disturbance. The step change in N_{en} is from 2500 to 3000 rpm. The throttle opening is 45° in all simulations. The results show that IMC performs well at all engine speeds, and it rejects the disturbance in N_{en}.

Next, the impact of the throttle opening u_{th} is considered. Two sets of tests are performed: the same P_b reference step at different throttle opening u_{th} (as in Fig. 15a), constant P_b reference with a step change in u_{th} (as in Fig. 15b), in which case the variation in u_{th} can be viewed as a disturbance. The step change in u_{th} is from 45 to 30°. The engine speed is 3000 rpm in all simulations. The results show that IMC performs well at all throttle openings, and it rejects the disturbance in u_{th}.

4.3. Discussion of applying IMC on turbocharged gasoline engine with CBV and EGR

A compressor bypass valve (CBV) is a valve that releases the boost pressure when the boost pressure is too high. It is commonly present in a turbocharged gasoline engine to prevent compressor surge. The proposed nonlinear IMC that is applicable to an engine with CBV. Generally, when the CBV dumps the boost pressure, by default the wastegate is set to be open, and the nonlinear IMC is disengaged. Therefore, the addition of CBV does not affect the nonlinear IMC design.

Exhaust gas recirculation (EGR) is a technique that involves a valve that recirculates a portion of exhaust gas back to the engine cylinders, which dilutes the air and reduces in-cylinder temperature. It can help reduce the NO_x emission. The engine discussed in this work has no EGR system. For an engine with EGR, the state-space equations (4) will be changed due to the coupling between the boost pressure and exhaust pressure dynamics with the presence of EGR. Therefore, the nonlinear model has to be revisited, and the parameters in the quasi-LPV model will change accordingly. The structured quasi-LPV inverse has to be reanalyzed. Application of nonlinear IMC to a turbocharged gasoline engine with EGR will be considered in future work.

5. Conclusions

A nonlinear IMC design for the turbocharged gasoline engine is presented. A nonlinear fourth-order dynamics model is adopted in the controller. The challenges for inverting the nonlinear model are addressed by: (1) representing the nonlinear dynamics with a quasi-LPV model, (2) exploring the special quasi-LPV model

structure, (3) using inverse of the simple first-order quasi-LPV model, and (4) assuring the stability of the inverse model by eliminating the internal loops. The simulation results, validated using a proprietary model as the "plant", demonstrate the validity of the proposed approach and establish the performance and robustness of the closed-loop system. The proposed nonlinear IMC presents a more implementable and less computationally expensive design than the other nonlinear IMC methodologies. It is however presented in the context of the boost pressure control of a turbocharged gasoline engine, and has not been generalized yet. Future work in this direction includes applying the nonlinear IMC to the boost pressure control of a plant with EGR and a real plant, expanding this specific nonlinear IMC design into a more general methodology, and developing a systematic approach for tuning the time constants.

References

Alfieri, E., Amstutz, A., & Guzzella, L. (2009). Gain-scheduled model-based feedback control of the air/fuel ratio in diesel engines. *Control Engineering Practice*, *17* (December (12)), 1417–1425.

Boukezzoula, R., Galichet, S., & Foulloy, L. (2000). Fuzzy nonlinear adaptive internal model control. *European Journal of Control*, *7*(December (5)), 541–556.

Brown, M. D., Lightbody, G., & Irwin, G. W. (1997). Nonlinear internal model control using local model networks. *Control Theory and Applications, IEE Proceedings*, *144*(November (6)), 505–514.

Buckland, J. H. (2009). *Estimation methods for turbocharged spark ignition engines* (Ph.D. dissertation). Ann Arbor, MI, USA: Department of Electrical Engineering and Computer Science, University of Michigan.

Calvet, J. P., & Arkun, Y. (1988). Feedforward and feedback linearization of nonlinear system and its implementation using internal model control (IMC). *Industrial & Engineering Chemistry Research*, *27*(10), 1822–1831.

Datta, A. (1998). *Adaptive internal model control*. London: Springer.

Economou, C. G., Morari, M., & Palsson, B. O. (1986). Internal model control: *Extension to nonlinear systems*. *Industrial & Engineering Chemistry Process Design and Development*, *25*(2), 403–411.

Garcia, C. E., & Morari, M. (1982). Internal model control. A unifying review and some new results. *Industrial & Engineering Chemistry Process Design and Development*, *21*(2), 308–323.

Guzzella, L., & Onder, C. H. (2010). *Introduction to modeling and control of internal combustion engine systems* (2nd ed.). Berlin, Heidelberg: Springer.

Henson, M. A., & Seborg, D. E. (1991). An internal model control strategy for nonlinear systems. *AIChE Journal*, *37*(July (7)), 1065–1081.

Hirschorn, R. M. (1979). Invertibility of nonlinear control systems. *SIAM Journal on Control and Optimization*, *17*(2), 289–297.

Hunt, K. J., & Sbarbaro, D. (1991). Neural networks for nonlinear internal model control. *Control Theory and Applications, IEE Proceedings D*, *138*(September (5)), 431–438.

Karnik, A., & Jankovic, M. (2012). IMC based wastegate control using a first-order model for turbocharged gasoline engine. In *American control conference* (*ACC*) (pp. 2872–2877), June.

Karnik, A. Y., Buckland, J. H., & Freudenberg, J. S. (2005). Electronic throttle and wastegate control for turbocharged gasoline engines. In *American control conference* (Vol. 7, pp. 4434–4439), June.

Mohammapour, J., Sun, J., Karnik, A., & Jankovic, M. (2013). Internal model control design for linear parameter varying systems. in *American control conference* (*ACC*) (pp. 2409–2414), June.

Morari, M., & Zafiriou, E. (1989). *Robust process control*. Englewood Cliffs, New Jersey: Prentice Hall.

Moulin, P., & Chauvin, J. (2011). Modeling and control of the air system of a turbocharged gasoline engine. *Control Engineering Practice*, *19*(March (3)), 287–297.

Qiu, Z., Sun, J., Jankovic, M., & Santillo, M. (2014). Nonlinear internal model controller design for wastegate control of a turbocharged gasoline engine. In *American control conference* (*ACC*) (pp. 214–219), June.

Rivera, D. E., Morari, M., & Skogestad, S. (1986). Internal model control: *PID controller design*. *Industrial & Engineering Chemistry Process Design and Development*, *25*(1), 252–265.

Rugh, W. J., & Shamma, J. S. (2000). Research on gain scheduling. *Automatica*, *36* (October (10)), 1401–1425.

Schwarzmann, D., Nitsche, R., & Lunze, J. (2006). Diesel boost pressure control using flatness-based internal model control. *SAE technical paper*, 2006-01-0855.

Schwarzmann, D., Nitsche, R., Lunze, J., & Schanz, A. (2006). Pressure control of a two-stage turbocharged diesel engine using a novel nonlinear IMC approach. In *Computer aided control system design*, *2006 IEEE international conference on control applications*, *2006 IEEE international symposium on intelligent control*, *2006 IEEE* (pp. 2399–2404), October.

Shafiq, M. (2005). Internal model control structure using adaptive inverse control strategy. *ISA Transactions*, *44*(July (3)), 353–362.

Thomasson, A., Eriksson, L., Leufven, O., & Andersson, P. (2009). Wastegate actuator modeling and model-based boost pressure control. In *IFAC workshop on engine and powertrain control*, *simulation and modeling* (Vol. 41).

Toivonen, H. T., Sandström, K. V., & Nyström, R. H. (2003). Internal model control of nonlinear systems described by velocity-based linearizations. *Journal of Process Control*, *13*(April (3)), 215–224.

Xie, W. F., & Rad, A. B. (2000). Fuzzy adaptive internal model control. *IEEE Transactions on Industrial Electronics*, *47*(February (1)), 193–202.